

Title: The Effect of Selected Sources on Broadband Delay Performance

Author: Bill Petrachenko

Date: Sept 7, 2006

Purpose:

The degree to which source structure degrades the ability to use broadband delay will be investigated. Five sources will be studied, and the analysis will be performed for 5 different frequency sequences.

Example Sources:

Complex visibilities for five randomly selected sources (Arthur Niell, IVS Memo 2006-018v01, "Source Structure Examples") were considered. The visibilities assume a 6,400 km baseline. Six baseline orientations were considered in increments of 30 degrees and the frequency coverage was between 1 and 16 GHz in increments of 0.1 GHz. The sources and their structure indices (SI) (Fey and Charlot, "VLBA Observations of Radio Reference Frame Sources. III. Astrometric Suitability of an Additional 225 Sources", ApJS, 128:17-83, 2000 May) are listed in Table 1.

Source	S-band SI	X-band SI
0014p813	1	1
0113m118	2	3
0149p218	2	2
0202p149	2	2
0248p430	2	4

Table 1. Example sources and their structure indices.

Example Frequency Sequences:

Five frequency sequences are considered. All bands have bandwidth 1 GHz and are completely filled. Three of the sequences were optimized with respect to their ability to resolve the RF phase at the lowest possible SNR. [An exhaustive search was performed in the range 2 to 15 GHz with step size 0.25 GHz.] The other two of the sequences use contiguous bands. Details of the sequences are listed in Table 2.

Name	Type	#bands	F1	F2	F3	F4	F5	F6	F7	F8
Seq4	Optimized	4	2.00	4.75	6.50	10.75				
Seq6	Optimized	6	2.00	3.50	4.75	7.50	9.50	12.00		
Seq6c	Contiguous	6	2.00	3.00	4.00	5.00	6.00	7.00		
Seq8	Optimized	8	2.00	3.25	4.50	5.50	6.50	9.00	13.00	14.00
Seq8c	Contiguous	8	3.00	4.00	5.00	6.00	7.00	8.00	9.00	10.00

Table 2. Example frequency sequences. All frequencies are in GHz and represent the lower edge of a 1 GHz band.

Delay Resolution Functions:

For frequency, ω_i , the complex point-source output of a VLBI correlator can be written,

$$A(\varpi_i) \cdot e^{j\phi(\varpi_i)}, \quad (1)$$

where $\phi(\varpi_i) = \varpi_i \cdot \tau - \frac{K}{\varpi_i}$,

τ is the dispersive part of the delay, and

K is a term proportional to the line-of-site electron content of the ionosphere.

Sources of dispersion other than the ionosphere may exist, but they will not be considered here. Also, typically, $A(\varpi_i)$ will vary somewhat with frequency due to variations of the system gain and atmosphere attenuation, but for the remainder of this discussion, it will be considered constant with frequency.

In order to integrate coherently across frequency, it is necessary to minimize the variation of the phase term. This can be done by removing a test phase of the form,

$$\phi^T(\varpi_i) = \varpi_i \cdot \tau^T - \frac{K^T}{\varpi_i}, \quad (2)$$

leaving a residual phase of the form,

$$\Delta\phi^T(\varpi_i) = \varpi_i \cdot \Delta\tau^T - \frac{\Delta K^T}{\varpi_i} \quad (3)$$

Summation can be done either over amplitude or the real component of the correlation coefficients, i.e. respectively,

$$\sum_i \left| A \cdot e^{j\Delta\phi(\varpi_i)} \right|, \quad (4)$$

$$\sum_i A \cdot \cos(\Delta\phi(\varpi_i)). \quad (5)$$

As $\Delta\tau$ and ΔK vary, the value of the summations will change. At the maximum of the functions, both $\Delta\tau$ and ΔK equal zero, and the test values of the parameters equal the observed values. In general, rates of change of these parameters also need to be considered; but, here, it will be assumed that the use of high bit rates along with burst mode data acquisition will make integration times short enough that this will not be necessary.

Concrete examples of the amplitude and cosine delay resolution functions are displayed in Figures 1 to 4 as grey scale plots. Amplitude resolution functions for Seq4 and Seq8c are displayed in Figures 1 and 3, while the corresponding cosine resolution functions are displayed in Figures 2 and 4. To reduce clutter and confusion in the plots, all structure below 0.4 of the variation has been removed and set to the white level. The circles in the plot represent target areas for determining if a fringe has been detected.

Amp ptrn: F=(2.00,4.75,6.50,10.75)

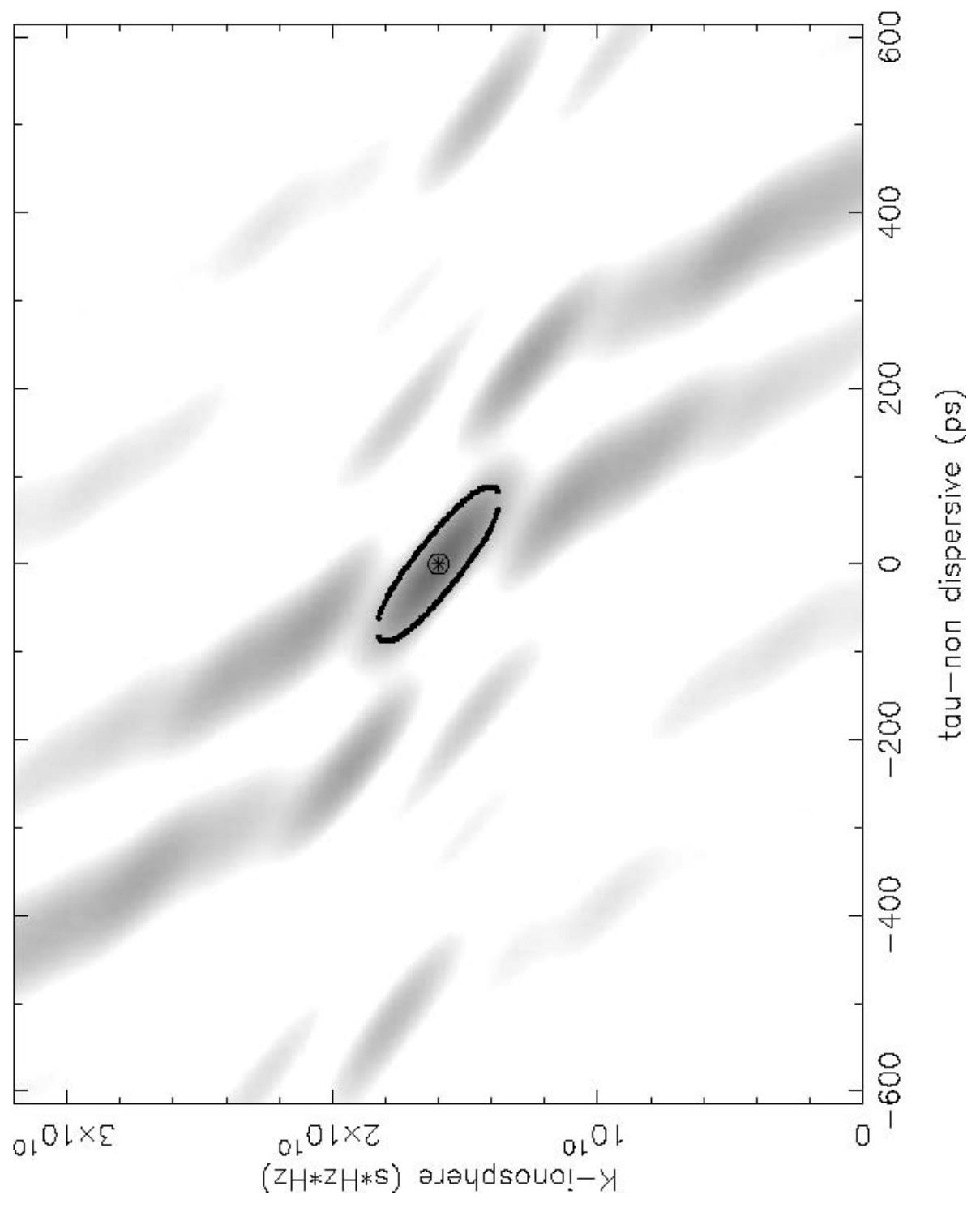


Figure 1. Amplitude resolution function for Seq4

Cos ptrn: $F=(2.00,4.75,6.50,10.75)$

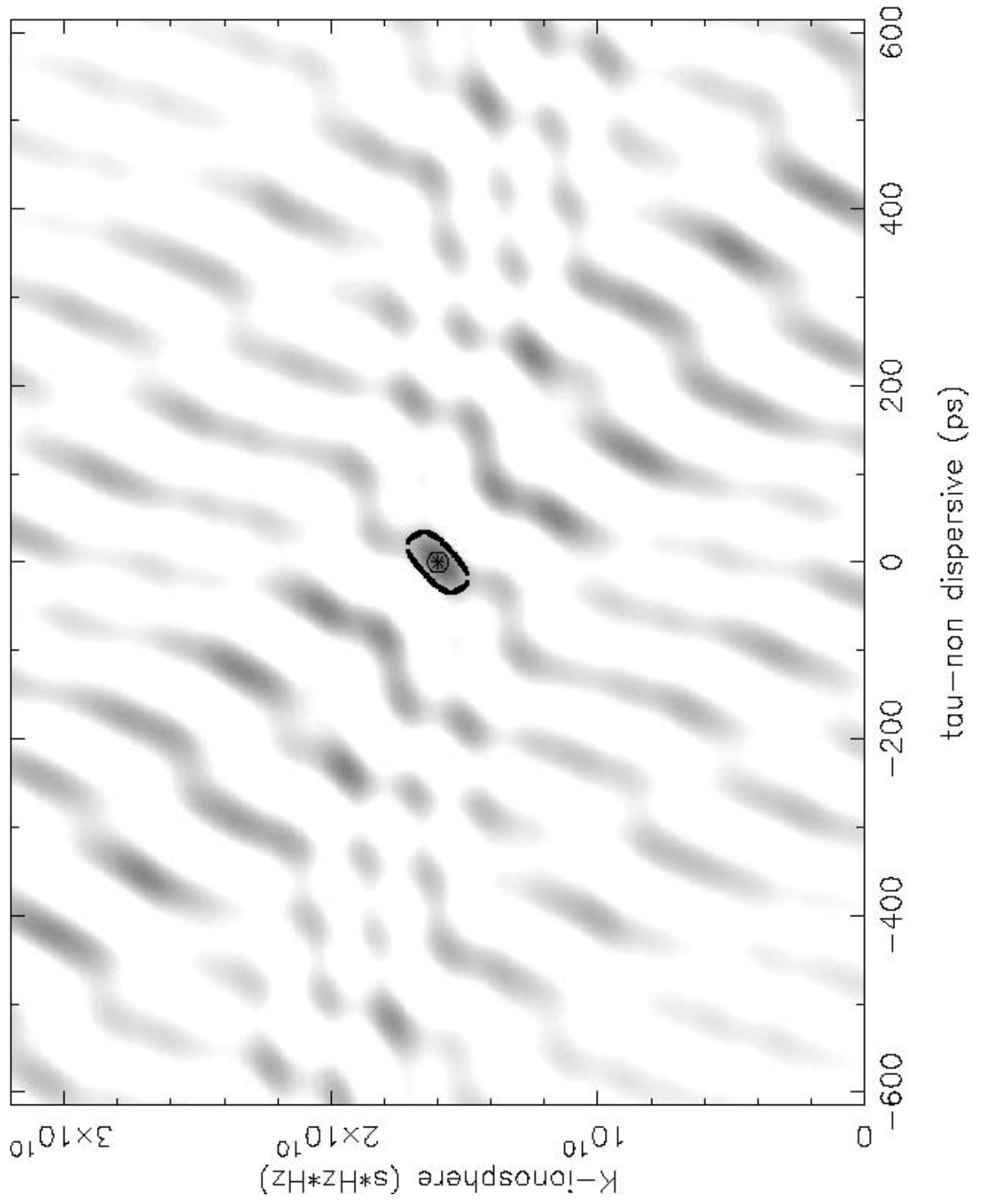


Figure 2. The cosine resolution function for Seq4.

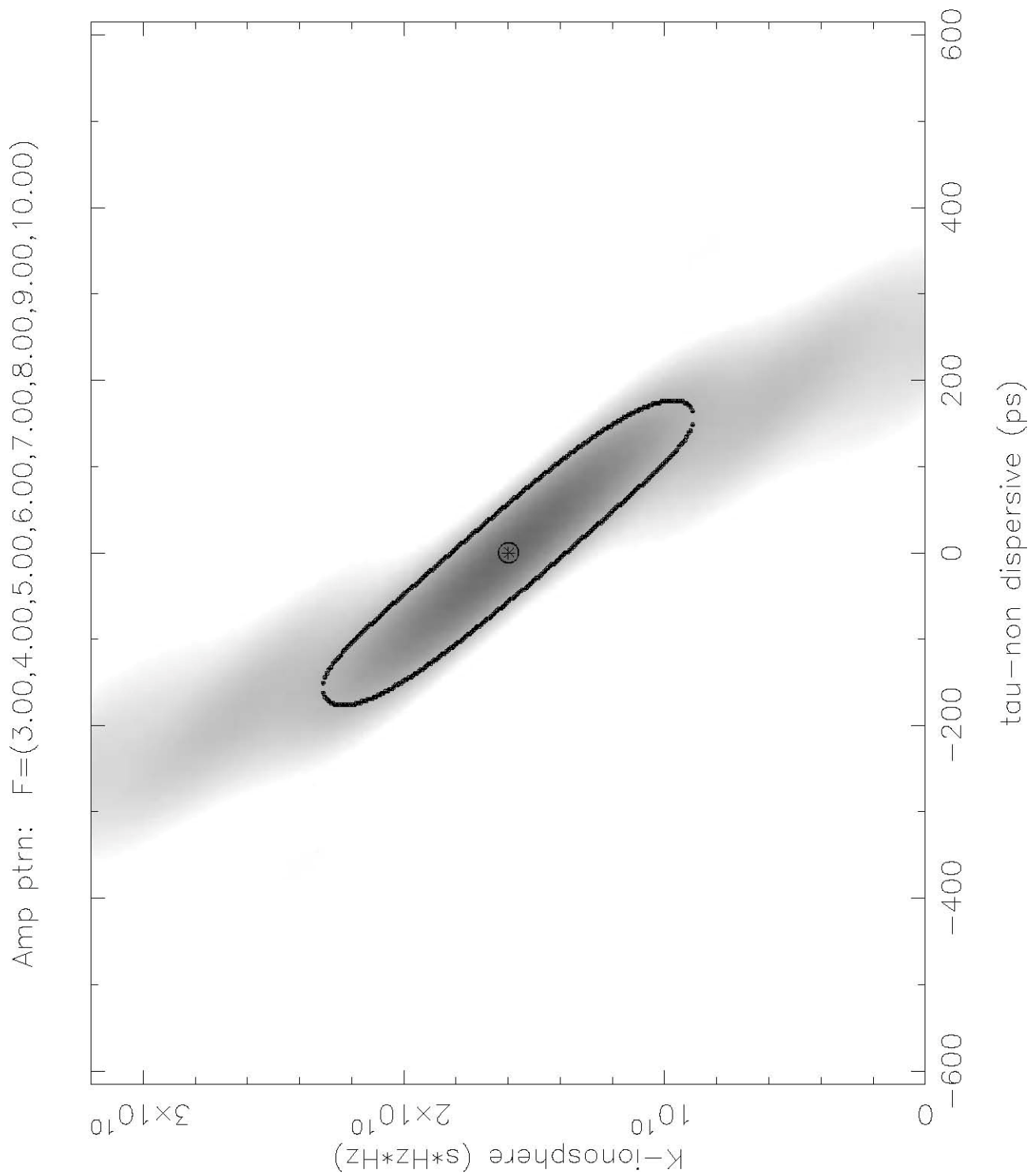


Figure 3. The amplitude resolution function for Seq8c

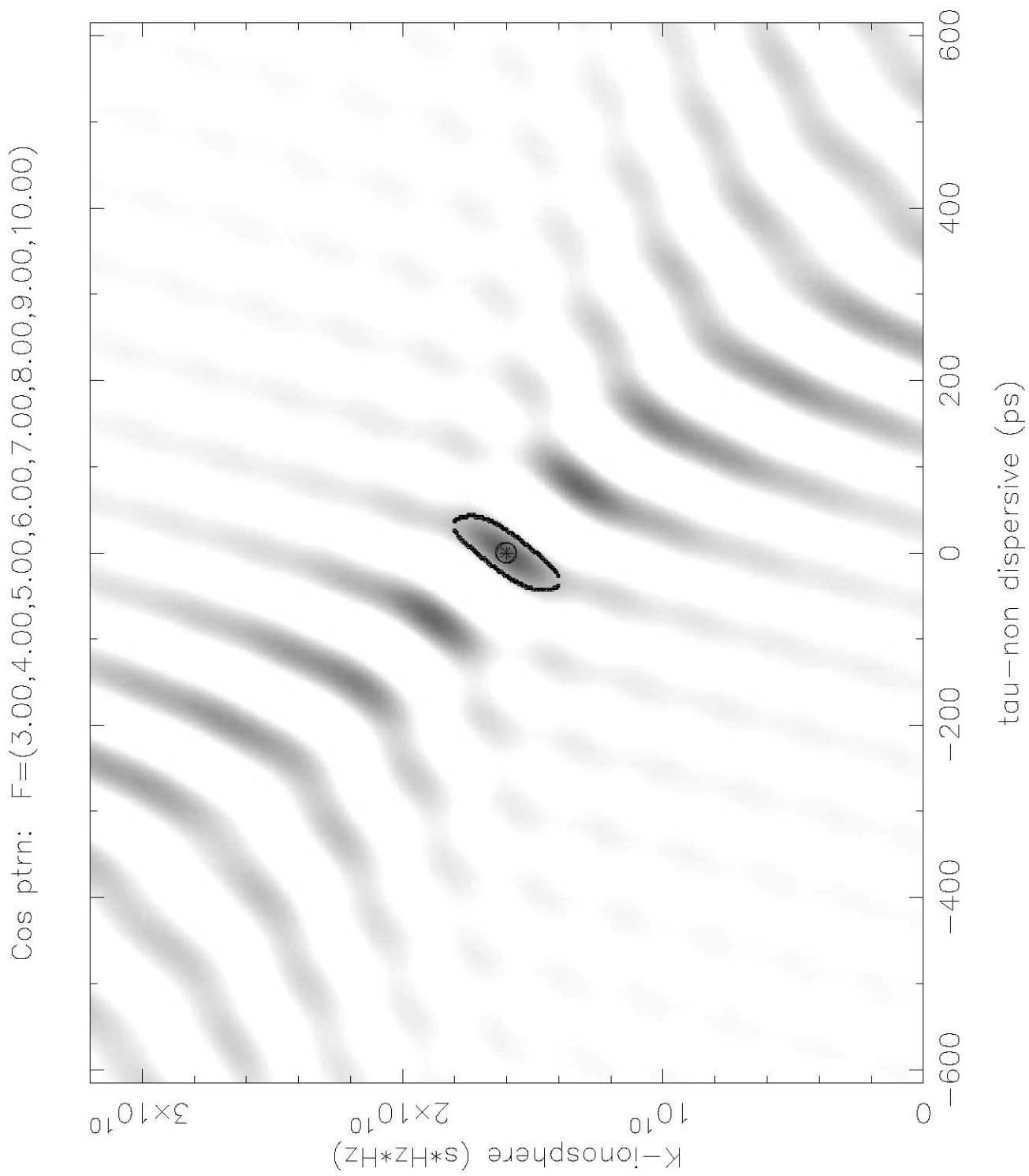


Figure 4. The cosine resolution function for Seq8c.

Effects of Source Structure on the Delay Resolution Function:

The effects of source structure can be incorporated by multiplying the point-source complex correlation coefficients by the complex visibilities provided by Arthur Niell, i.e.

$$\left(A \cdot e^{j\phi(\varpi_i)} \right) \cdot \left(A_S(\varpi_i) \cdot e^{j\phi_S(\varpi_i)} \right) \quad (6)$$

The amplitude and cosine delay resolution function (assuming Seq4) for source 0014p813 (orientation 0 degrees) are displayed in Figures 5 and 6 respectively. This source has a structure index of (1,1), which is the best in the list. It was chosen since the effect of structure is least likely to be noticeable. As expected, the effects are difficult to detect.

The amplitude and cosine delay resolution function (assuming Seq4) for source 0248p430 (orientation 0 degrees) are displayed in Figures 7 and 8 respectively. This source has a structure index of (2,4), which is the worst in the list. It was chosen since the effect of structure is most likely to be noticeable. Note that, in addition to other troublesome structure changes (such as a double amplitude peak), the peak of the amplitude plot has been offset from the nominal by 123 ps, and the peak of the cosine plot has been offset by 147 ps.

Amp ptrn: F=(2.00,4.75,6.50,10.75)

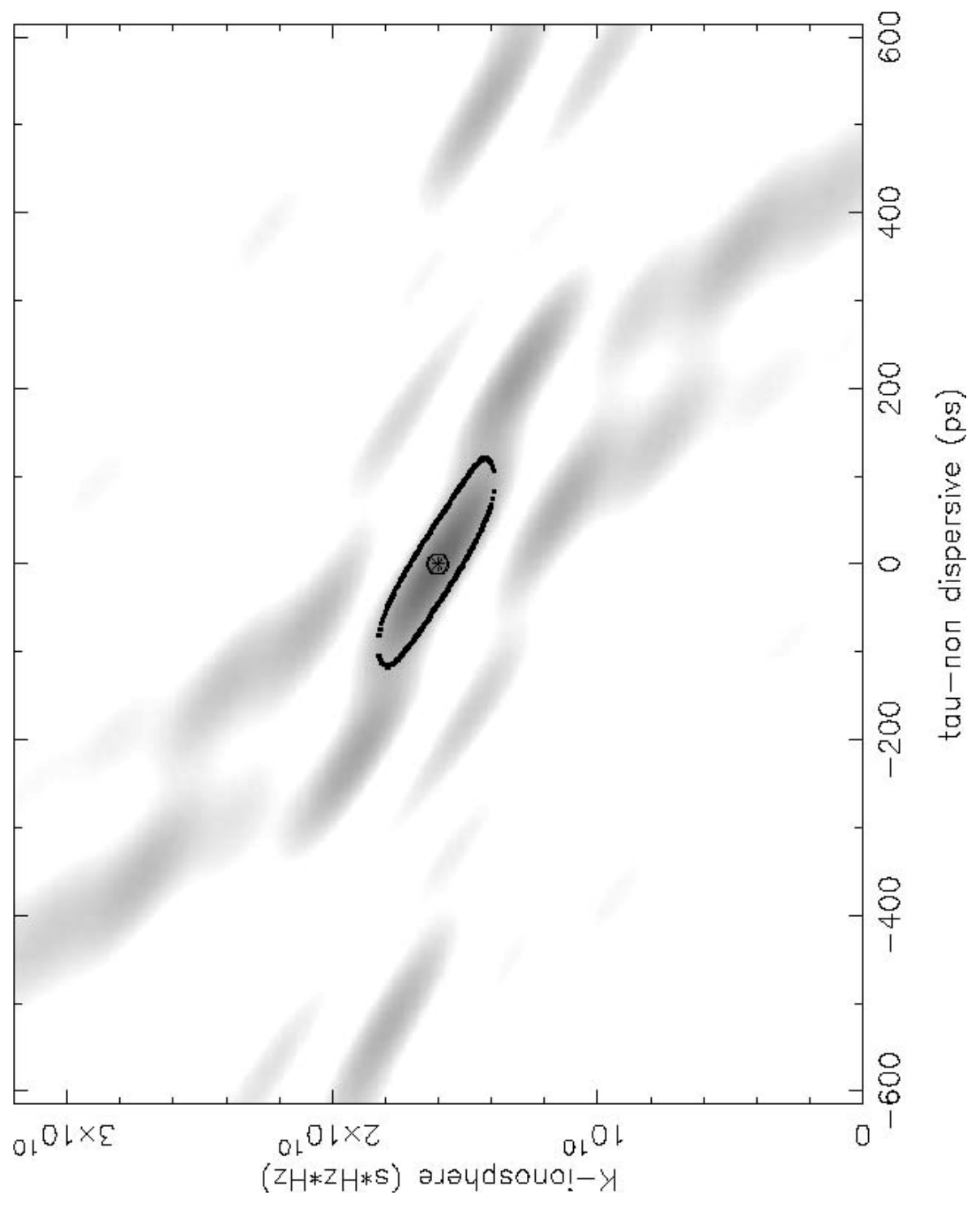


Figure 5. The amplitude delay resolution function (Seq4) for 0014p813.

Cos ptrn: F=(2.00,4.75,6.50,10.75)

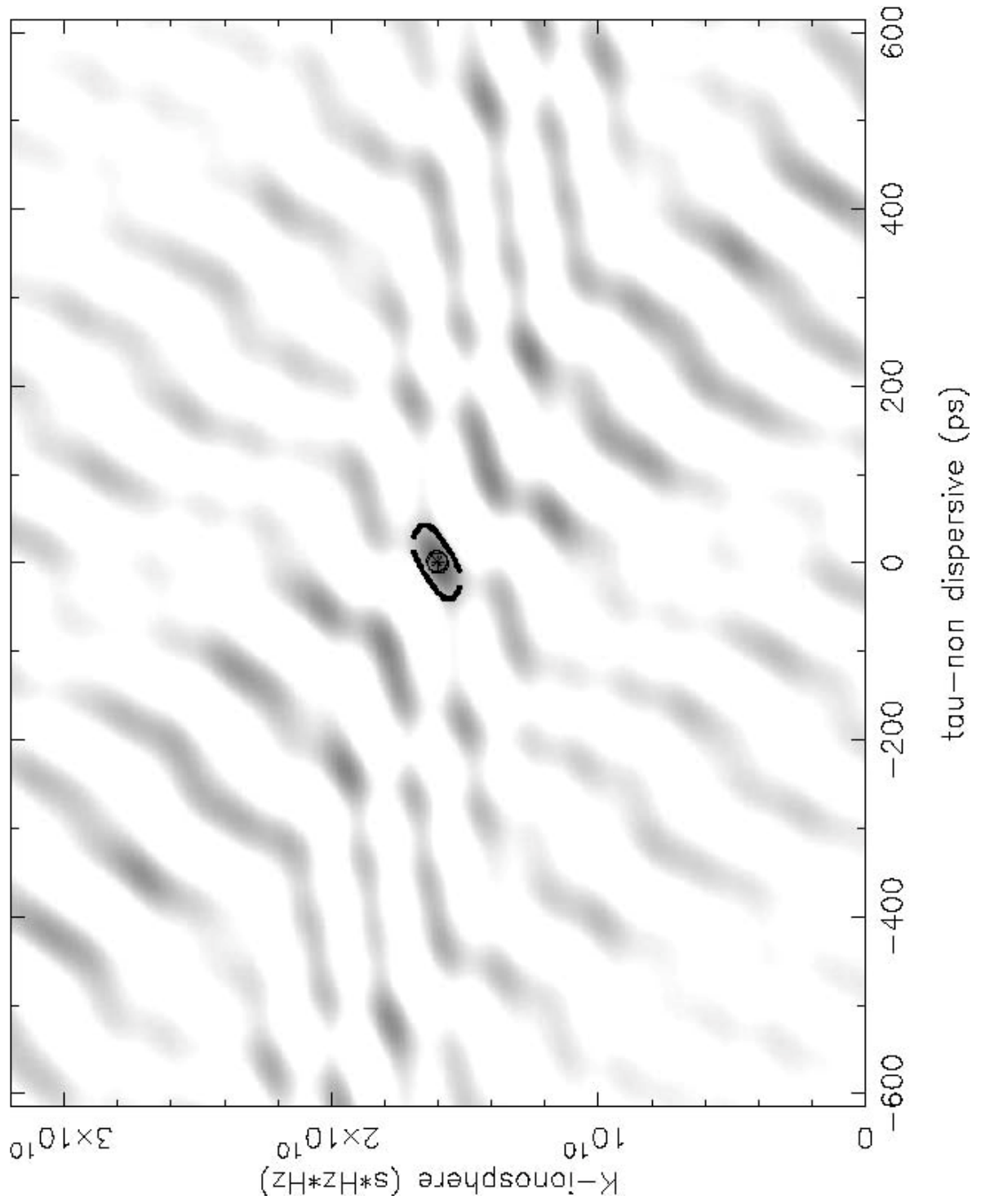


Figure 6. The cosine delay resolution function (Seq4) for 0014p813.

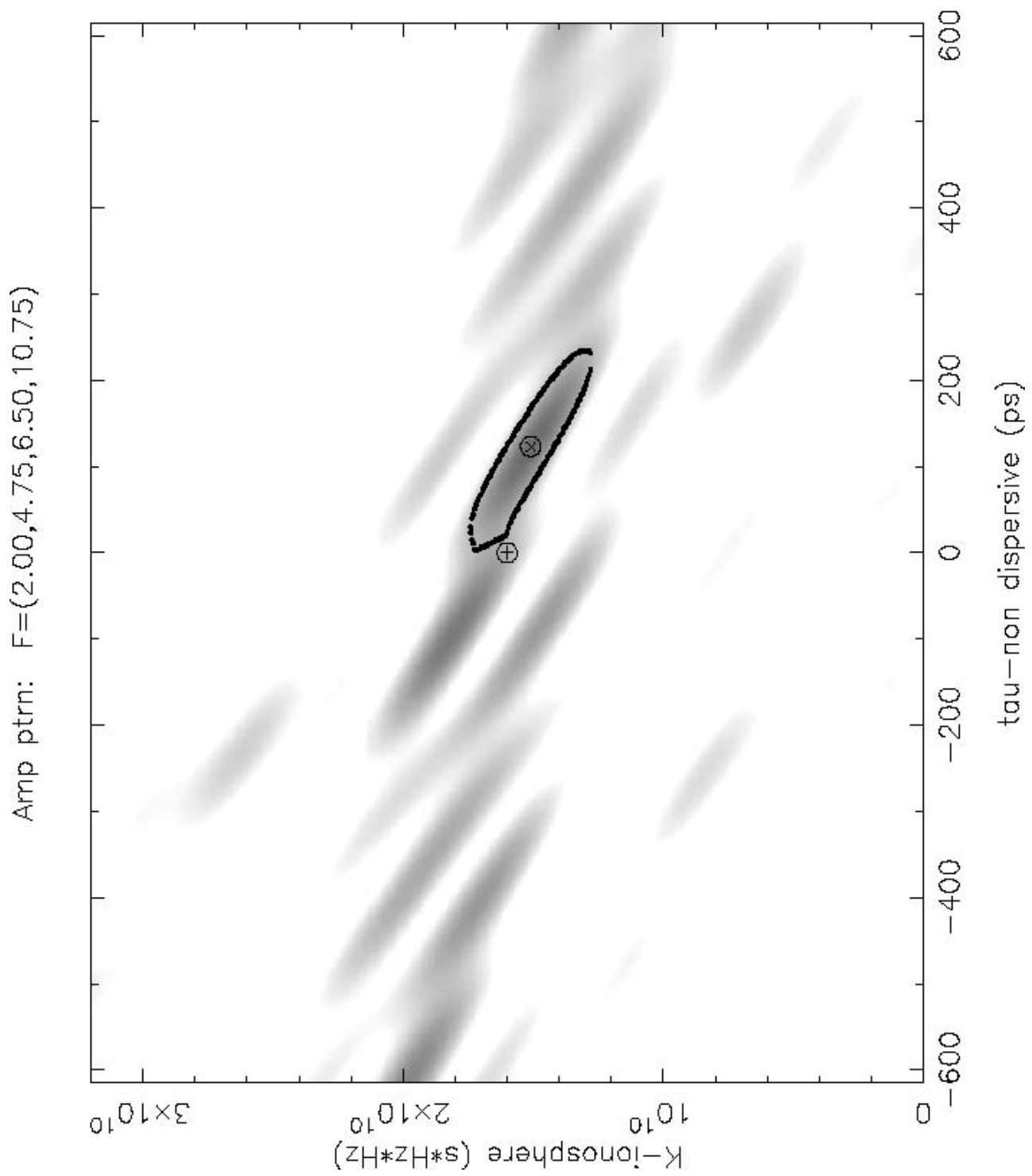


Figure 7. The amplitude delay resolution function (Seq4) for 0248p430.

Cos ptrn: F=(2.00,4.75,6.50,10.75)

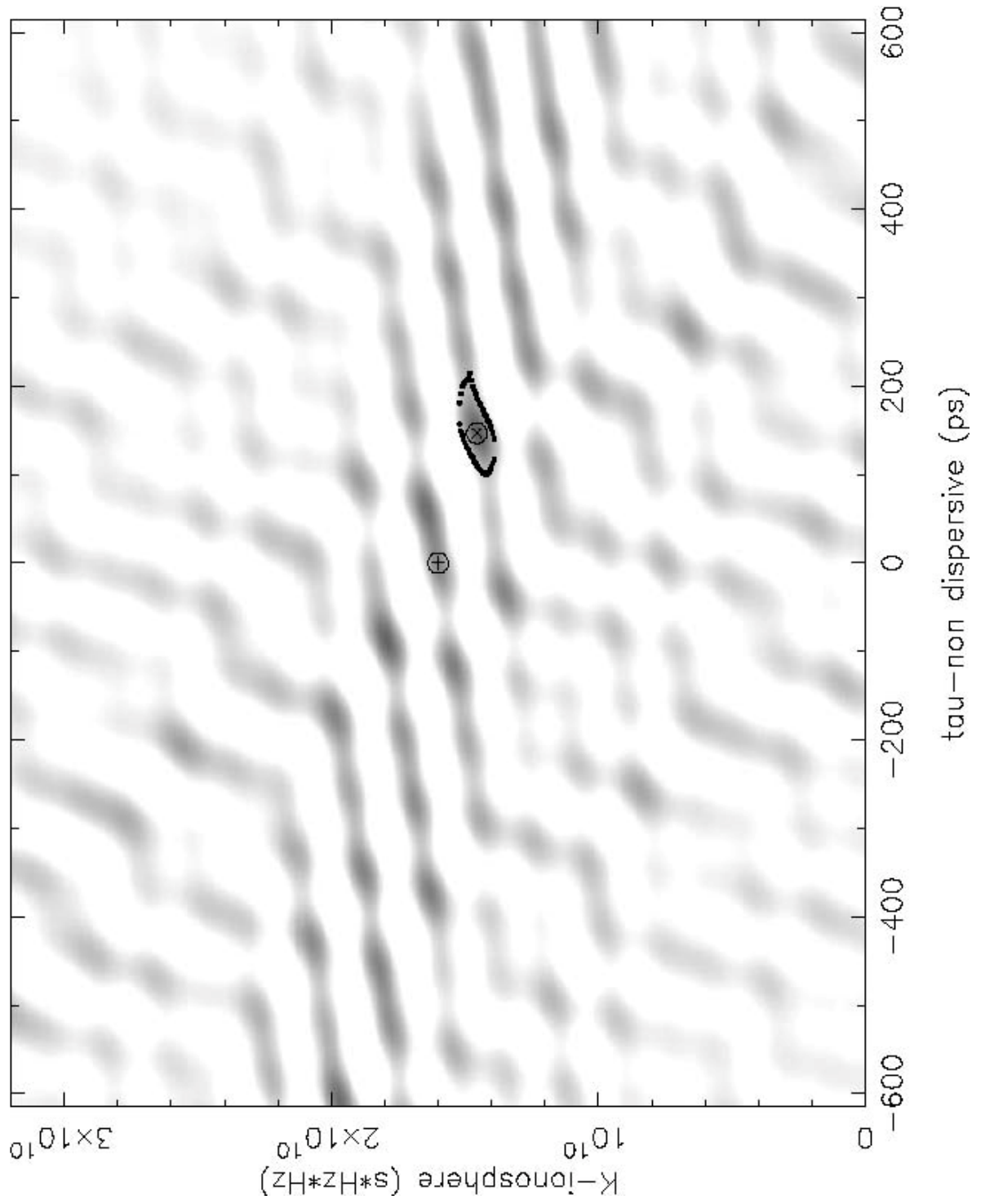


Figure 8. The cosine delay resolution function (Seq4) for 0248p430.

Monte Carlo Analysis:

A statistical simulation study was performed to see how well τ and K might be recovered from correlator output. Each sample of the ensemble was generated in the following way:

- Random values of τ and K were selected within a specified region.
- Correlation coefficients were generated according to Equation 1 for a specified frequency sequence. The separation of frequency points was 25 MHz, which produced 40 points in each 1 GHz band.
- Source structure was incorporated into the correlation coefficients according to Equation 6.
- Noise was added to the correlation coefficients to achieve a specified overall SNR.
- A coarse search of the amplitude pattern was performed using Equations 2, 3 and 4. The search increments were $0.2 / f_{\max}$ and $0.2 \cdot f_{\min}^2$ for τ and K respectively.
- The maximum of the coarse search values was used as the starting point for a fine search to the peak of the amplitude pattern. This produced the recovered values of τ and K for that pattern.
- The values of τ and K from the amplitude fine search were then used to perform a fine search of the cosine pattern (Equation 5). This produced the recovered values of τ and K for that pattern.

Using this procedure, an ensemble of recovered values of τ and K was generated for both the amplitude and the cosine patterns. Statistical analysis was then performed on these ensembles.

In Figures 9 and 10, the ensemble values (1000 samples) for a point source with SNR=8 are plotted on their respective amplitude and cosine patterns. At an overall SNR of 8, the error rate is about 3%. An SNR of 8 was selected so that the distribution of blunder points could be seen. As expected, they are found at high points of the delay resolution function.

In Figures 11 and 12, the ensemble values (1000 samples) for 0248p430 (structure index (2,4)) with SNR=24 are plotted on their respective amplitude and cosine patterns. Because the delay resolution function has been degraded by the visibility function of 0248p430, at an overall SNR of 24, the error rate is about 6%. Because there is a second lobe of the delay resolution function that is nearly as high as the maximum, it takes a higher SNR to get unambiguous amplitude and phase resolution.

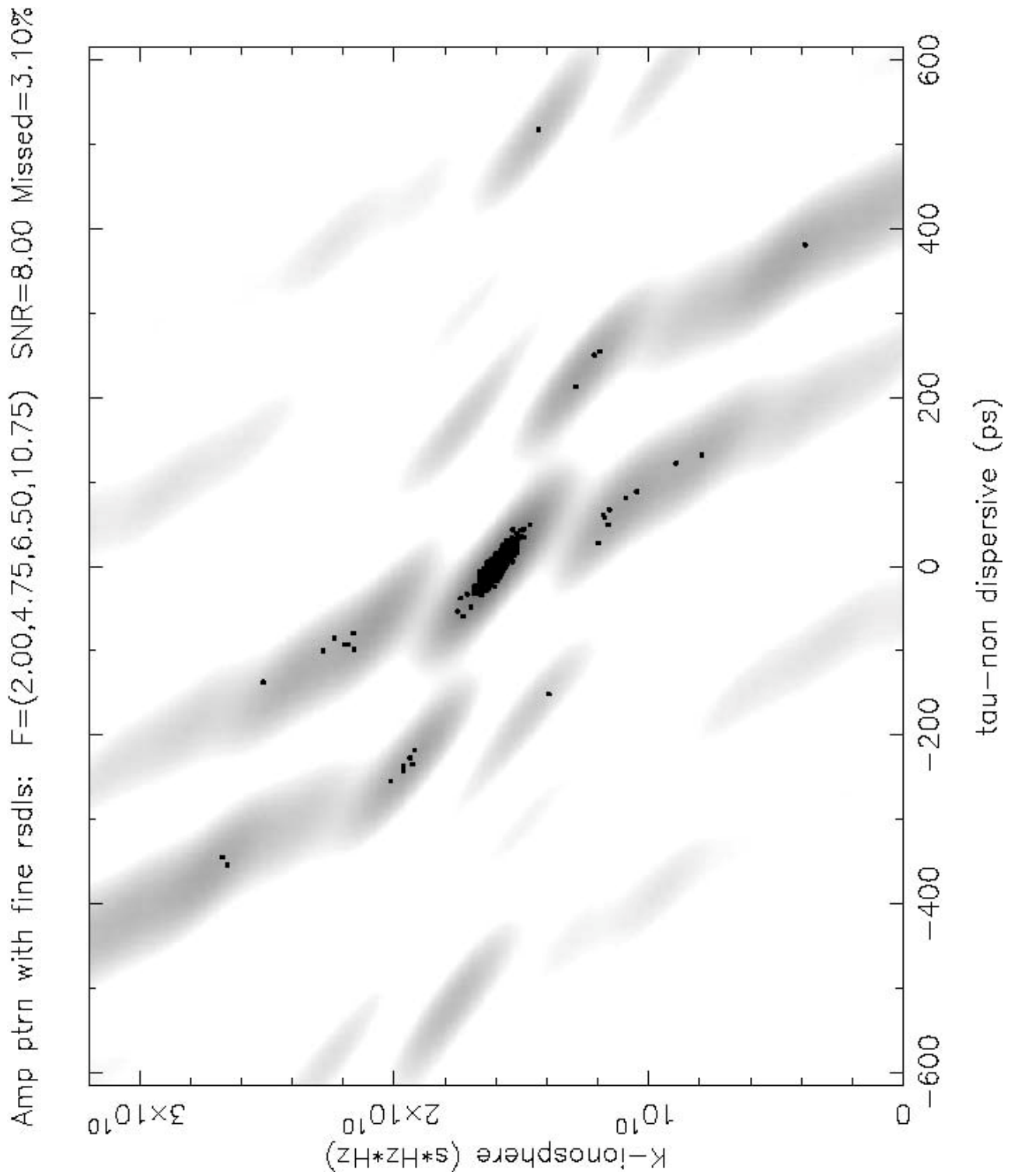


Figure 9. The ensemble values (1000 samples) for a point source with SNR=8 plotted on the amplitude delay resolution function.

Cos ptrn with phase rsdls: F=(2.00,4.75,6.50,10.75) SNR=8.00 Missed=3.60%

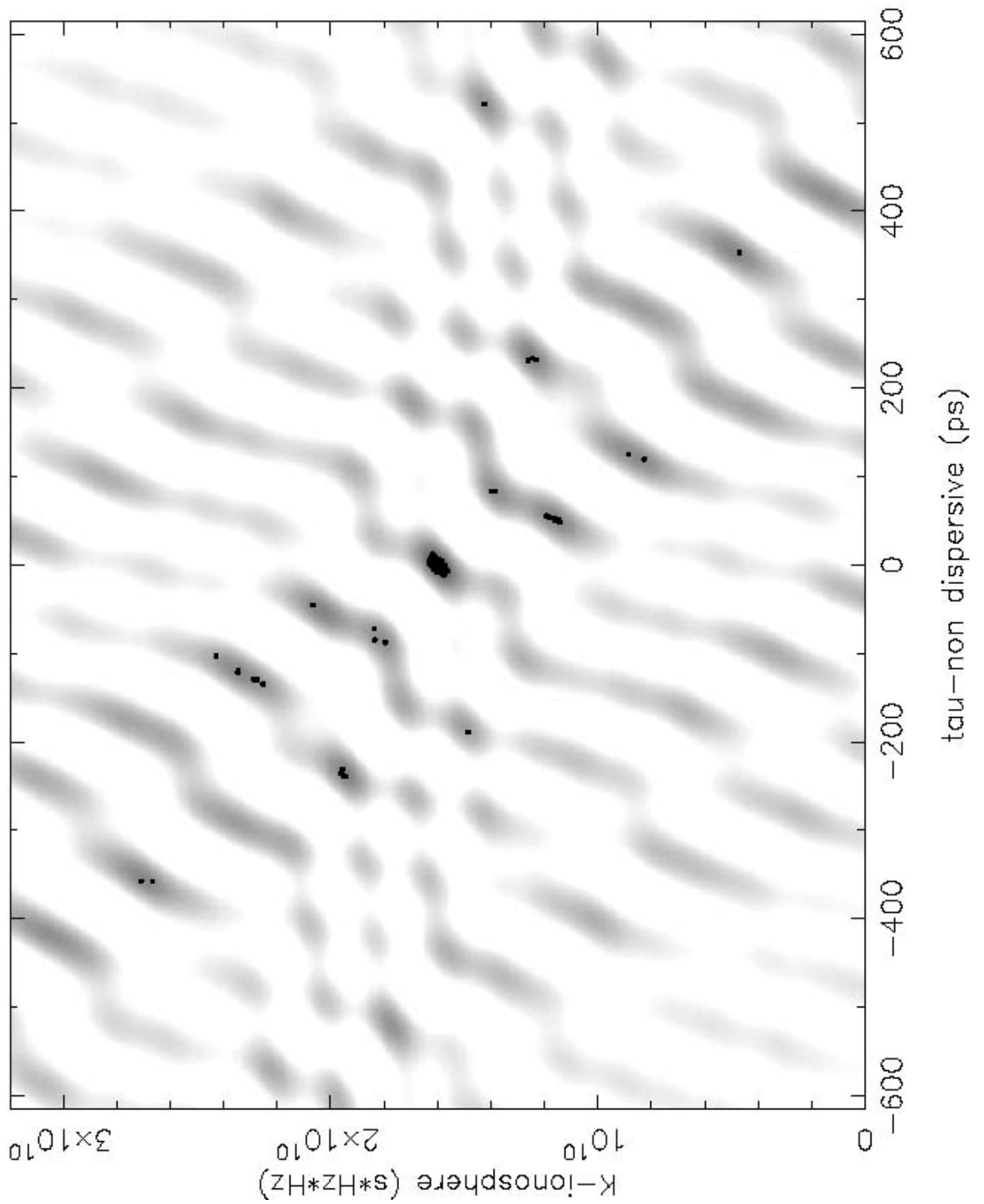


Figure 10. The ensemble values (1000 samples) for a point source with SNR=8 plotted on the cosine delay resolution function.

Amp ptrn with fine rsdls: F=(2.00,4.75,6.50,10.75) SNR=24.00 Missed=6.10%

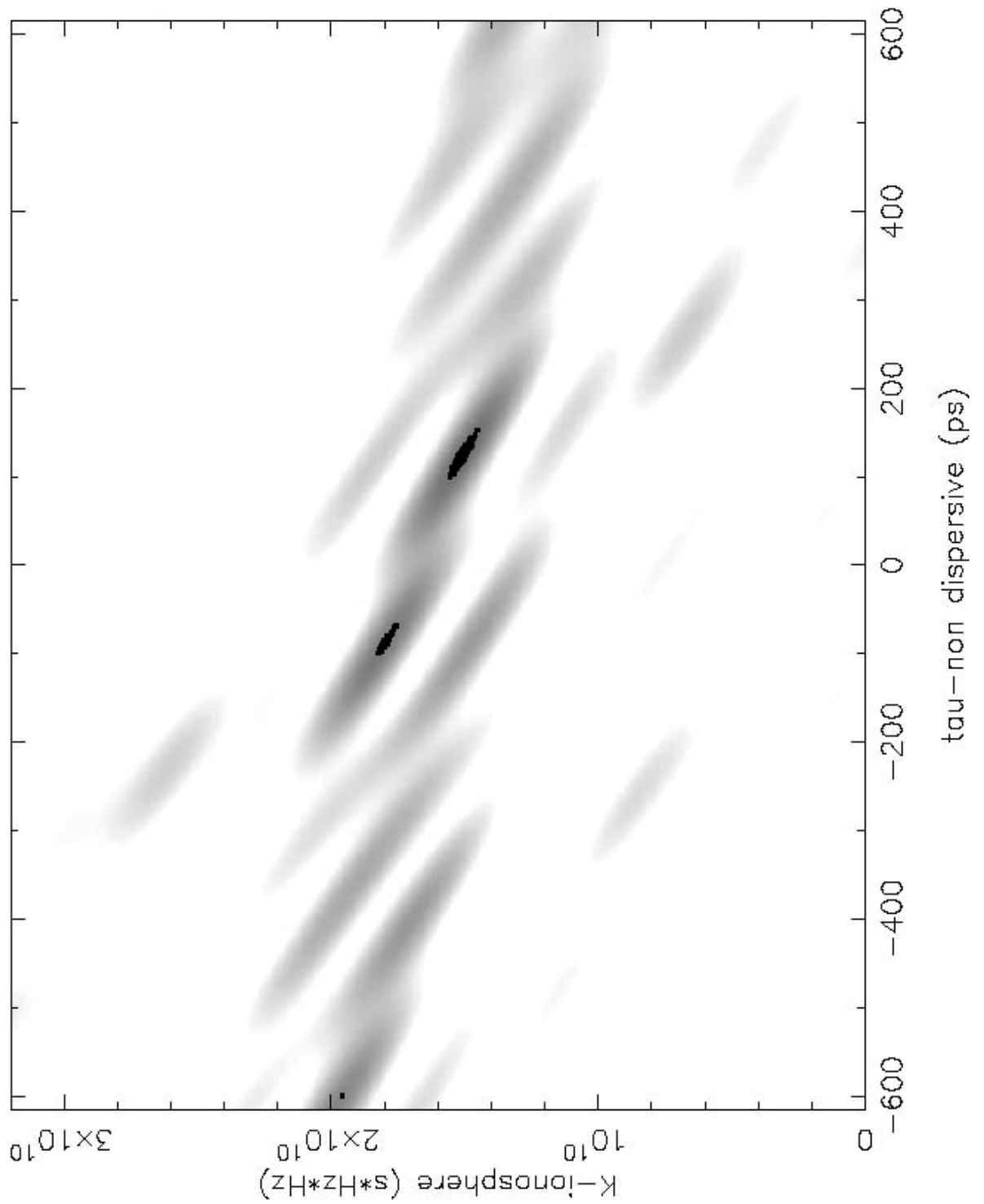


Figure 11. The ensemble values (1000 samples) for 0248p430 with SNR=8 plotted on the amplitude delay resolution function.

Cos ptrn with phase rsdls: F=(2.00,4.75,6.50,10.75) SNR=24.00 Missed=6.30%

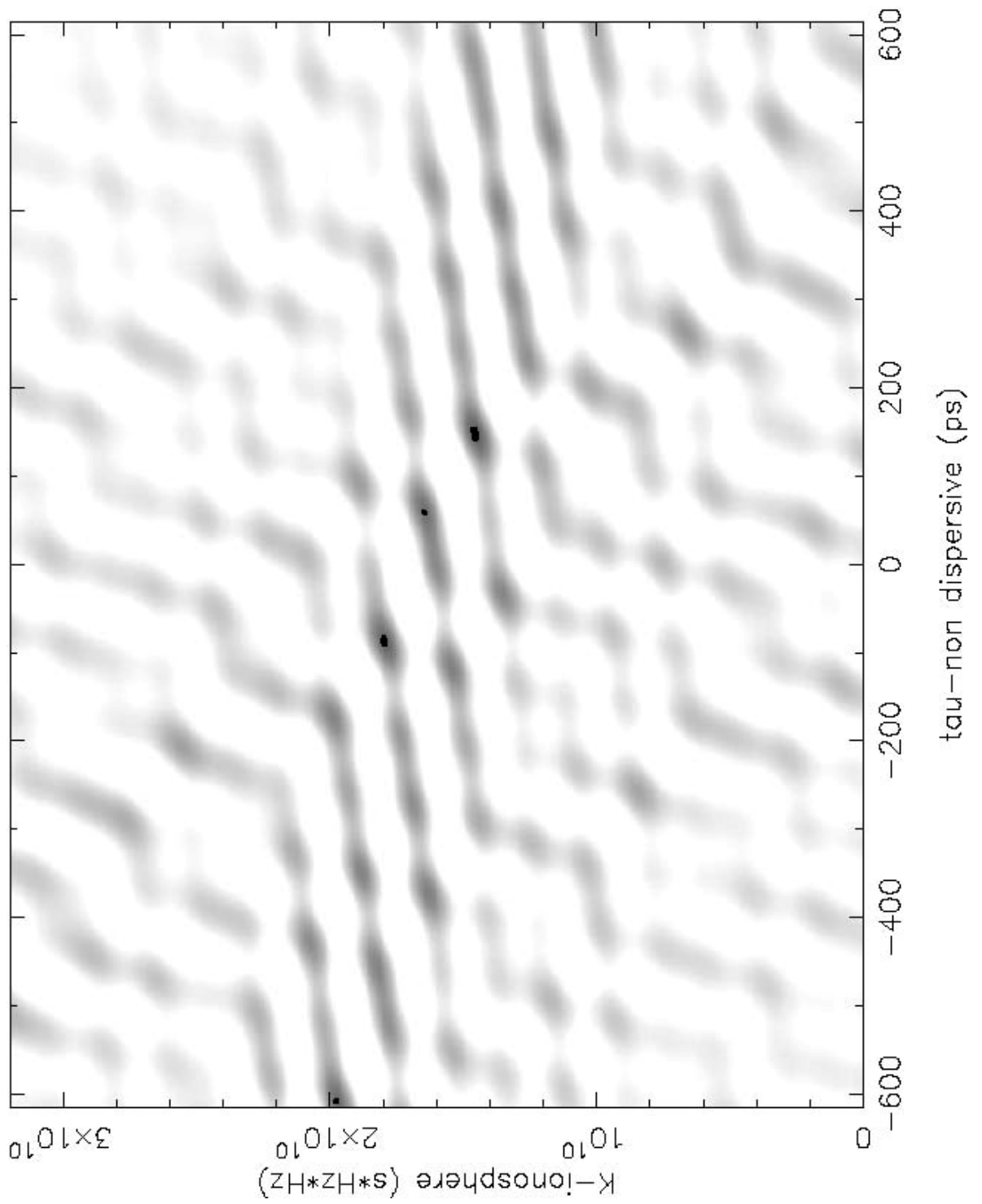


Figure 12. The ensemble values (1000 samples) for 0248p430 with SNR=8 plotted on the cosine delay resolution function.

Results for Different Sources:

The results using Seq4 for all sources and all 6400 km baseline angles have been summarized in Table 3:

- The column labeled 'Amp Offset' represents the τ offset (ps) of the peak of the amplitude delay resolution function from its nominal value.
- The column labeled 'Cosine Offset' represents the τ offset (ps) of the peak of the cosine delay resolution function from its nominal value.
- The column labeled 'Amp SNR' represents the SNR at which the blunder rate for a sample of 1000 amplitude searches drops to 0.
- The column labeled 'Cosine SNR' represents the SNR at which the blunder rate for a sample of 1000 cosine searches drops to 0.
- The column labeled 'Amp rms' represents the rms scatter of 1000 τ values (ps) determined in an amplitude search.
- The column labeled 'Cosine rms' represents the rms scatter of 1000 τ values (ps) determined in a cosine search.

It is clear from the table that, at least for the sources selected for this study, sources with structure index less than (2,2) will perform very well with respect to the use of broadband delay, while sources at or above (2,3) will only be useable if meaningful source structure corrections can be applied.

Source Name	Bsln Angle	Amp Offset	Cosine Offset	Amp SNR	Cosine SNR	Amp rms	Cosine Rms
point src	0	0	-0.1	12.25	11.25	8.89	2.36
0248p430 (2,4)	0	123.1	147.9	46.2	47.6	14.4	6.2
	30	-56.5	-11.9	42.3	121.0	34.8	12.3
	60	8.0	3.1	12.9	18.2	19.6	4.3
	90	-143.0	-143.9	47.5	50.0	15.8	5.6
	120	131.7	163.8	157.1	153.1	17.1	5.1
	150	122.9	163.4	19.8	85.0	19.8	5.4
0202p149 (2,2)	0	-0.6	0.4	10.4	10.4	11.5	2.9
	30	0.5	-0.7	10.9	10.5	9.8	2.7
	60	0.5	0.6	10.3	9.9	9.4	2.4
	90	1.7	0.1	11.0	11.7	10.7	2.8
	120	0.6	0.9	13.4	11.9	13.5	3.5
	150	1.2	-0.1	12.6	12.8	15.1	3.6
0149p218 (2,2)	0	-2.2	0.0	10.9	11.4	11.8	2.9
	30	0.8	0.6	12.3	12.3	10.9	2.9
	60	1.2	-0.2	9.5	9.9	10.0	2.6
	90	-3.7	0.9	11.6	11.6	9.6	2.7
	120	-1.4	-0.1	11.3	12.9	11.2	3.0
	150	1.8	0.1	11.4	13.0	11.4	2.9
0113m118 (2,3)	0	25.1	-2.5	47.0	53.9	14.1	3.5
	30	-47.1	-74.8	31.5	75.2	16.7	2.2
	60	-2.8	-3.4	11.0	13.8	12.0	3.4

	90	176.8	159.0	67e6	67e6	----	----
	120	8.8	4.6	27.0	29.8	15.1	3.2
	150	-24.3	-0.5	110.7	94.2	15.1	5.8
0014p813 (1,1)	0	-0.5	0.9	12.5	12.8	13.4	3.6
	30	1.3	0.8	11.7	13.2	13.9	3.6
	60	1.5	0.2	10.3	11.3	11.2	3.0
	90	-4.0	0.3	11.0	11.4	10.1	2.6
	120	0.2	0.6	11.4	12.6	9.7	2.8
	150	-1.8	0.2	10.1	12.3	12.0	3.0

Table 3. Results for all sources using Seq4.

Results for different frequency sequences:

The results using all frequency sequences with respect to both a point source and 0248p430 (SI (2,4)) have been summarized in Table 4:

- The column labeled ‘Amp Offset’ represents the τ offset (ps) of the peak of the amplitude delay resolution function from its nominal value.
- The column labeled ‘Cosine Offset’ represents the τ offset (ps) of the peak of the cosine delay resolution function from its nominal value.
- The column labeled ‘Amp SNR’ represents the SNR at which the blunder rate for a sample of 1000 amplitude searches drops to 0.
- The column labeled ‘Cosine SNR’ represents the SNR at which the blunder rate for a sample of 1000 cosine searches drops to 0.
- The column labeled ‘Amp rms’ represents the rms scatter of 1000 τ values (ps) determined in an amplitude search.
- The column labeled ‘Cosine rms’ represents the rms scatter of 1000 τ values (ps) determined in a cosine search.

For the point source, the optimized sequences, Seq4, Seq6 and Seq8, worked better than the contiguous sequences. Seq6 and Seq8 worked somewhat better than Seq4, but the differences were not that great.

For a poorly behaved source like 0248p430 (SI (2,4)), it is more difficult to discern a consistent pattern. Subjectively, the best and worst sequences for each baseline angle are summarized in Table 5. According to this criterion, the contiguous sequences typically work better than the optimized sequences.

Source Name	Bsln Angle	Sequence Name	Amp Offset	Cosine Offset	Amp SNR	Cosine SNR	Amp Rms	Cosine rms
point	0	4	0.0	0.1	12.3	11.3	8.6	2.3
		6	-0.1	0.1	9.3	9.8	8.4	2.2
		6c	0.4	0.1	9.3	15.3	22.8	4.1
		8	-0.3	0.0	10.3	9.3	6.4	1.8
		8c	0.4	0.1	9.8	20.3	18.1	3.2
0248p430	0	4	123.1	147.9	46.2	47.6	14.4	6.2
		6	-78.5	-92.1	46.9	44.4	15.9	3.1
		6c	75.1	30.3	20.2	71.5	24.4	10.6

		8	182.0	170.2	214.7	185.4	17.8	6.3
		8c	-143.8	-155.8	19.3	24.8	19.6	2.7
0248p430	30	4	-56.5	-11.9	42.3	121.0	34.8	12.3
		6	-54.8	-14.7	12.4	67.8	26.2	12.4
		6c	-17.4	-6.7	8.7	19.0	24.2	4.9
		8	-73.9	-109.7	47.8	69.6	13.0	5.2
		8c	-50.4	-15.0	14.5	135.8	31.8	4.9
0248p430	60	4	8.0	3.1	12.9	18.2	19.6	4.3
		6	6.0	3.2	11.8	16.6	16.9	4.1
		6c	18.8	3.0	8.1	23.1	22.6	4.4
		8	-12.6	-1.1	28.8	32.3	17.6	5.0
		8c	17.4	6.8	7.7	27.5	22.1	4.4
0248p430	90	4	-143.0	-143.9	47.5	50.0	15.8	5.6
		6	59.5	93.5	37.8	71.7	16.1	6.1
		6c	-78.1	-133.7	12.3	2265.1	109.5	11.3
		8	-47.1	-25.0	79.6	88.4	13.8	6.5
		8c	109.8	76.0	9.8	100.8	18.9	3.3
0248p430	120	4	131.7	163.8	157.1	153.1	17.1	5.1
		6	177.6	212.0	45.9	52.1	12.9	3.8
		6c	125.6	105.3	11.4	30.4	27.0	6.0
		8	176.1	208.6	16.4	46.4	9.7	3.9
		8c	212.5	209.0	10.6	25.2	24.2	4.6
0248p430	150	4	122.9	163.4	19.8	85.0	19.8	5.4
		6	181.4	212.1	44.6	51.7	12.7	3.7
		6c	128.2	105.4	16.1	29.1	28.5	5.9
		8	176.5	208.5	21.9	43.3	8.7	3.6
		8c	218.9	209.1	12.1	28.9	22.2	4.3

Table 4. Results for different sequences using either a point source or 0248p430

Baseline Angle	Best Sequence	Worst Sequence
0	8c	8
30	6c	4
60	6	8
90	4	6c
120	8c	4
150	8c	6

Table 5. Best and worst sequences for each baseline angle of 0248p430

Conclusions:

At least for the sources selected for this study, those with structure index less than (2,2) perform very well with respect to the use of broadband delay, while sources at or above structure index (2,3) perform very poorly and may be unusable without source structure corrections. This is encouraging. The distribution of structure indexes for the 230 sources in the third Fey/Charlot survey (Fey and Charlot, "VLBA Observations of Radio Reference Frame Sources. III. Astrometric Suitability of an Additional 225 Sources",

ApJS, 128:17-83, 2000 May) are listed in Table 6. About 60% of sources are below structure index (2,2). If this distribution holds more or less for the remaining sources of the ICRF, then roughly 400 sources should be available for use with broadband delay. The large position offsets associated with sources of structure indices (2,3) and above make them undesirable anyway. However, before drawing any firm conclusions, more sources below structure index (2,2) need to be studied.

S-band SI	X-band SI	# of Sources	% of Sources
1	1	46	20.0
1	2	67	29.1
1	3	26	11.3
1	4	8	3.5
2	1	3	1.3
2	2	21	9.1
2	3	24	10.4
2	4	8	3.5
3	1	0	0.0
3	2	2	0.9
3	3	12	5.2
3	4	10	4.3
4	1	0	0.0
4	2	0	0.0
4	3	0	0.0
4	4	3	1.3

Table 6. Distribution of Structure Indices

As far as sequences are concerned, for sources with low structure indices, the optimized sequences, Seq4, Seq6 and Seq8, work somewhat better than the contiguous sequences. For sources with high structure indices, the contiguous sequences appear to be somewhat more robust, but it is anticipated that few of these sources will be scheduled for observation.